MIJST
MIST International Journal of Science and Technology

Importance of Stress and Temperature-Dependent Permeability of Rocks and its Application in Underground Nuclear Waste Disposal

AKM Badrul Alam[1*], Yoshiaki Fujii[2], Nahid Hasan Dipu[3], Boeurt Sophea[4] and Afikah Binti Rahim[5]

[1,3]Department of Petroleum and Mining Engineering, Military Institute of Science and Technology, Dhaka, Bangladesh
[2]Faculty of Engineering, Hokkaido University, Sapporo, Japan
[4]Research Unit of Materials Science and Structure, Institute of Technology of Cambodia, Phnom Penh, Cambodia
[5]School of Civil Engineering, Universiti Teknologi Malaysia, 81310, Johor Bahru, Johor, Malaysia

emails: *[1]rock.mist.badrul18@gmail.com; [2]fujii6299@ymail.ne.jp; [3]nahiddipu2@gmail.com; [4]boeurtsophea@gmail.com; and [5]afikahrahim@utm.my*

ARTICLE INFO

Article History:

Received: 07th March 2023
Revised: 14th May 2023
Accepted: 14th May 2023
Published: 25th June 2023

Keywords:

Rock-permeability
Stress and temperature dependent-permeability
Water inflow
Underground nuclear waste disposal cavern

ABSTRACT

Water flow is an essential factor in the sealability of any underground cavern, including those for nuclear waste disposal, and is significantly affected by the permeability of the rock. The permeability of rocks is affected by various factors, including stress and temperature. The rock stress changes by excavating a cavern, and rock temperature changes by decay heat from nuclear waste, and the temperature change induces thermal stress. Therefore, water flow around such caverns must be evaluated considering the effects of stress and temperature. Numerical analyses of water migration around underground nuclear waste disposal caverns have been carried out. However, studies considering the stress and temperature-dependent permeability may not be published yet. To demonstrate the necessity to consider the stress and temperature-dependency in permeability, equations that represent the post-failure permeability as a function of average effective stress and temperature were proposed. The water inflow was numerically calculated for a simple underground nuclear waste disposal cavern with or without stress and temperature dependency which showed the significance of the dependency. Also, the importance of rock types was demonstrated by considering the three rocks of granite, sandstone, and tuff for a full-scale underground radioactive disposal site for the stress and temperature-dependent permeability. A high sealability could be expected for granite and sandstone but not for the tuff. Introducing the stress and temperature-dependent permeability could contribute to the thoughtful design of an underground repository for radioactive waste disposal considering rock types.

1. INTRODUCTION

In the sealability of any underground cavern, including those for nuclear waste disposal, water flow is an essential factor. It is significantly controlled by the permeability of the rock. The permeability of rocks is affected by various factors, including stress and temperature. For example, the results of a series of permeability measurements for three rock types under confining pressure between 1 - 14 MPa at 22°C/ 295 K and 80°C/ 353 K were given by Alam *et al.* (2014 and 2015). The excavation of a cavern changes the rock stress and decay heat from cesium, strontium, americium, curium etc. in nuclear waste changes the rock temperature. The thermal stress is induced by the temperature change (Figure 1). Therefore, water flow around such caverns must be evaluated considering the stress and temperature effects. Numerical analyses of water migration around underground nuclear waste disposal caverns have been carried out. For example, Bian *et al.* (2012) numerically calculated the thermo-hydromechanical behavior of the surrounding rock mass of micro tunnels for high-level nuclear waste disposal in Callovo-Oxfordian claystone formation by FLAC3D, which is a commercial code adapting fast Lagrangian analysis provided by Itasca Consulting Group using finite-difference method (FDM).

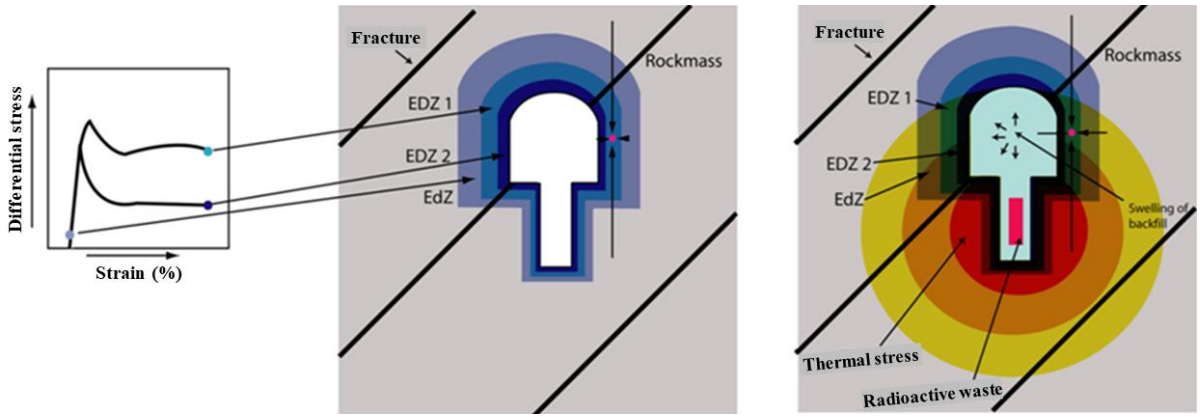

Figure 1: Conceptual model of temperature, thermal stress in EDZ and EdZ around an underground nuclear waste disposal cavern (Alam *et al.*, 2015)

Kwon *et al.* (2013) studied thermal stress distribution around canisters containing nuclear wastes and applied the solutions to consider bentonite inclusions by FLAC3D. Yu *et al.* (2017) derived analytical solutions for thermo-hydro-mechanical behavior of rock mass around a heating hole and PRACLAY and ATALS III heating tests—however, none of these studies considered the stress and temperature-dependent permeability.

This paper does not aim to perform a detailed thermo-hydro-mechanical numerical analysis for a specific site's rock mass but to show the general importance of taking into account the stress and temperature dependency in the water migration analyses around underground nuclear waste disposal caverns and how to apply it in a mined-repository for nuclear waste. First, we propose equations describing post-failure permeability as a function of average effective stress and temperature based on Alam *et al.* (2015)'s experimental results. The post-failure permeability here refers to the permeability of rocks that have fractured and reached the residual strength state. Rock masses are fractured and have much higher permeability than intact rocks. The difference in permeability between rock masses and post-failure rocks is likely to be much smaller than that between rock masses and intact rocks. It can also be said that measuring the post-failure rock's permeability is much more feasible than measuring the intact rock's permeability because the former is much higher than the latter, primarily for hard rocks. We then calculate the water migration into a simple underground nuclear disposal cavern with a 2-D elastic FEM (Finite Element Method) and explain the results. Based on these results, we present the water inflow around the underground repository for radioactive waste considering the potential of radio nuclide migration by groundwater, showing the importance of rock type.

2. MATERIALS AND METHODS

For the experiment, Inada granite, Kimachi sandstone, and Shikotsu welded tuff were selected, covering a wide range of rock physical properties (Table 1). The commercially available intact rock blocks were used for the experiments. The Shikotsu welded tuff from Hokkaido, Japan, contains plagioclase, hypersthene, augite, hornblende, and transparent glass. All these minerals are relatively small in grain size. The grains of each mineral were smaller than 1 mm.

The Miocene Kimachi sandstone from Shimane, Japan, has mostly andesite rock fragments and some minerals like plagioclase, pyroxene, hornblende, biotite, and quartz. The matrix also has calcium carbonate, iron oxides, and zeolites. It is a clastic rock with good-sorting grains sizing about 0.4–1.0 mm (Dhakal *et al.*, 2002).

The main minerals in the Paleocene Inada granite from Ibaraki, Japan, are quartz, feldspar, biotite, and allanite. It also has some zircon, apatite, and ilmenite (Lin *et al.*, 2008). The minerals have different grain sizes: quartz is about 3.0–4.0 mm, plagioclase and alkali feldspar are about 2.0–3.0 mm, and biotite is usually smaller than 1.0 mm.

Table 1
Physical properties of rocks. *γ: Dry density, φ: Effective porosity, UCS: Uniaxial compressive strength (saturated) (Alam et al., 2015*)

Rock type	γ (g/cm^3)	φ (%)	*UCS* (MPa)
Shikotsu welded tuff	1.30±0.01 (*n*=10)	35.6±1.7 (*n*=2)	13.53±2.74 (*n*=2)
Kimachi sandstone	1.98±1.01 (*n*=13)	18.4±2.0 (*n*=2)	20.53±2.35 (*n*=2)
Inada granite	2.70±0.01 (*n*=17)	0.63±0.05 (*n*=2)	180.85±16.93 (*n*=2)

Inada granite has the lowest effective porosity of less than 1% and the highest water-saturated uniaxial compressive strength ($UCS_{water\text{-}saturated}$) of 181 MPa. While the Shikotsu welded tuff has a high effective porosity of 37% and 14 MPa, it has the lowest water-saturated uniaxial compressive strength. On the other hand, Kimachi sandstone has a $UCS_{water\text{-}saturated}$ of 21 MPa and an effective porosity of 19%.

The specimens, which were 30 mm in diameter and 60 mm long, were fully saturated in de-ionized water in a water-submersible vacuum jar before two stainless steel

endpieces were taped to the saturated specimen. A hole was drilled through the center of each endpiece for water flow to the specimen. A layer of silicone sealant prevents the water from flowing inside the specimen. The specimen and the associated endpieces were then covered with a heat-shrinkable tube to prevent the confined fluid from permeating into the specimen. The sample was then immersed for 24 hours in de-ionized water.

The samples were put in a triaxial cell (Alam *et al.*, 2014) with a heater and a controller around them (Figure 2). The tests were done at 22°C/ 295 K or 80°C/ 353 K with different pressures from all sides (1–15 MPa). The pressure values matched the pressure from the weight of the rock above them between 58–814 m deep. We assumed that the rock was fully saturated and weighed 27 kN/m^3 and that the water level was at the ground level. The highest temperature (80°C) was what we expected for the rock around a nuclear waste site (Kwon *et al.* 2013). It was also the highest temperature that the triaxial cell could handle.

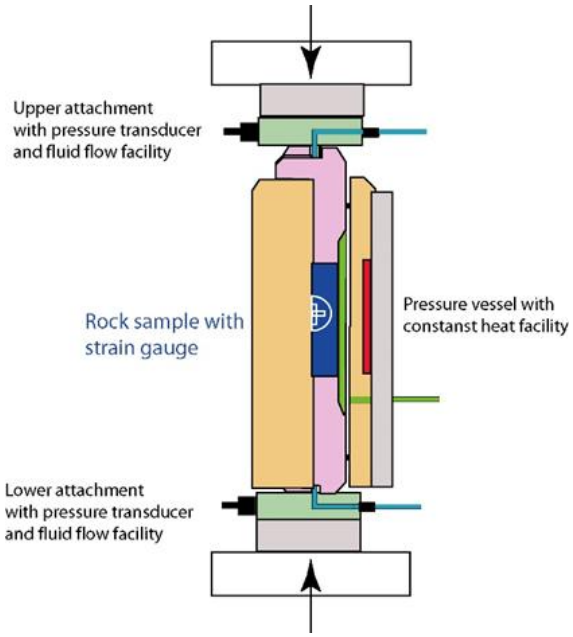

Figure 2: Triaxial vessel with heat facility

A screw-type Instron 5586 loading frame was used for loading. Syringe pumps were used to apply confining pressure and pore pressure.

Following consolidation, a steady compression rate of 10^{-5} s^{-1}, or 0.036 mm/min, was used to increase the strain until it reached 10% for Shikotsu welded tuff or 7% for Kimachi sandstone and Inada granite. To attain the stable residual strength state, high strain values were used.

We used different methods to measure the permeability of three types of rocks. For Shikotsu welded tuff, we applied the constant flow method. While for Kimachi sandstone and Inada granite, the transient-pulse method with Brace *et al.*'s (1968) approximate solution was used. We recorded the load, stroke, pore pressure, confining pressure, and flow rate every 10 s on a data logger during the experiment. Micrographs from blue-resin-infused specimens were prepared to observe the structural changes under stress and temperature.

3. POST-COMPRESSION ROCKS AND THE PERMEABILITY

A. Micrographs of Post-Compression Rocks

The rock specimens of post-compression were saturated in blue resin to observe the pores and fractures. Afterward, the microscopic slides were prepared from the blue-resin-infused specimens by using mineralogic slide preparation units performing cutting, grinding and polishing. The blue colors in the micro-graphs represent the open spaces.

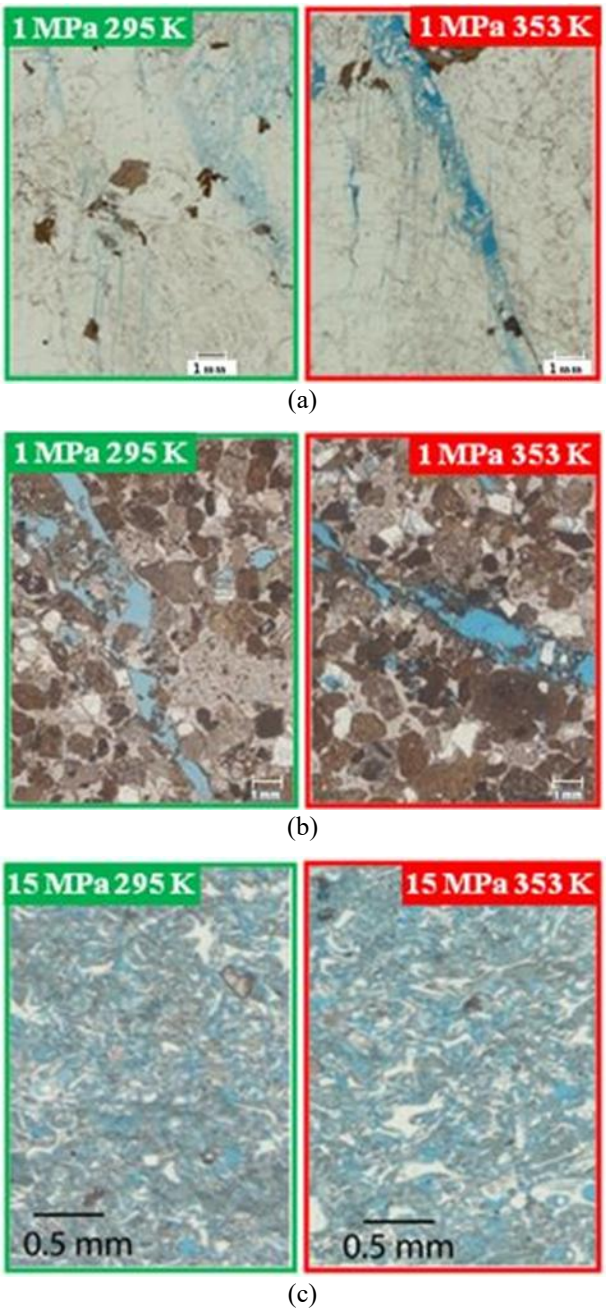

Figure 3: Micrographs after compression at confining pressures in increased temperature, (a) Inada granite, (b) Kimachi sandstone, and (c) Shikotsu welded tuff

In Inada granite, broad rupture planes with a network of microcracks were observed at a lower confining pressure of 1 MPa at 295 K. The comprehensive network of microcracks in rupture planes at 1 MPa 295 K and the network is narrower for 1 MPa 353 K in Inada granite

(Figure 3). In contrast, a wide rupture plane with larger pores (approx. 1 mm) was observed at 1 MPa 295 K, which is narrow with small pores (approx. less than 0.5 mm) at 1 MPa 353 K in Kimachi sandstone (Figure 3). The number of pores was higher at 15 MPa 295 K than at 15 MPa 353 K in Shikotsu welded tuff (Figure 3).

B. *Post-Failure Permeability of Rocks as a Function of Stress and Temperature*

As shown in Figure 4, the permeability after failure was inversely related to average effective stress (AES, σ', MPa), which was derived from Equation (1) using the residual strength (σ), pore pressure (P_p), and confining pressure (P_c).

$$\sigma' = \frac{\sigma+2P_C}{3} - P_p \quad (1)$$

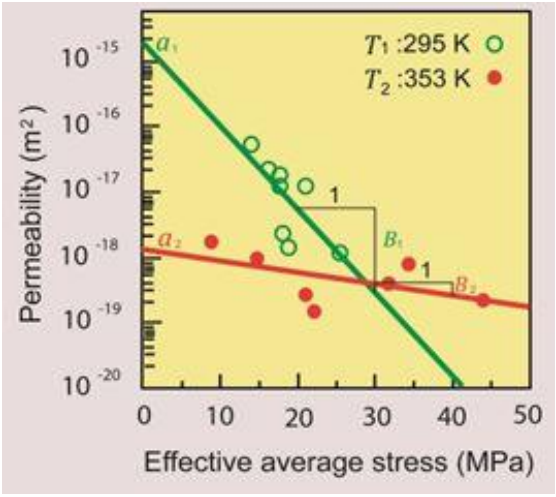

Figure 4: Temperature and stress effects on permeability in Inada granite

Shikotsu welded tuff and Inada granite had higher and more stress-sensitive permeability after failure at 295K (K_1) than at 353K (K_2). However, for Kimachi sandstone, the permeability difference was slight, and the stress dependency was similar at both temperatures. The equations below show the relationship between the permeability and the σ' for rocks.

$$log\ K_1 = A_1 + B_1\sigma'\ at\ T_1 \quad (2)$$

$$log\ K_2 = A_2 + B_2\sigma'\ at\ T_2 \quad (3)$$

$$A_1 = log\ a_1 \quad (4)$$

$$A_2 = log\ a_2 \quad (5)$$

Here a_i is the regression line's y-intercept, and B_i is the stress sensitivity at T_i (Figure 5). Temperature influences on permeability A (-), B (MPa^{-1}) can be seen in the differences between a_1 (permeability at T_1 under σ' = 0) and a_2 (permeability at T_2 under σ' = 0) or between B_1 and B_2. Compared to sandstone, they are significantly more prominent for granite and tuff (Figure 5, Table 2). Equations (6 to 8) were derived assuming linear correlations between temperature and the constants to represent the stress and temperature-dependent permeability K.

$$K = 10^{A+B\,\sigma'} \quad (6)$$

$$A = A_1 + \frac{T-T_1}{T_2-T_1}(A_2-A_1) \quad (7)$$

$$B = B_1 + \frac{T-T_1}{T_2-T_1}(B_2-B_1) \quad (8)$$

Table 2
Permeability at 295K (a_1) and 353K (a_2), stress dependency at 295K (B_1), and 353K (B_2)

Rock type	a_1 (m²)	a_2 (m²)	B_1 (MPa^{-1})	B_2 (MPa^{-1})
Shikotsu welded tuff	5.43×10^{-15}	4.91×10^{-16}	-0.041	-0.013
Kimachi sandstone	1.25×10^{-17}	8.00×10^{-18}	-0.034	-0.043
Inada granite	1.72×10^{-15}	1.22×10^{-18}	-0.127	-0.036

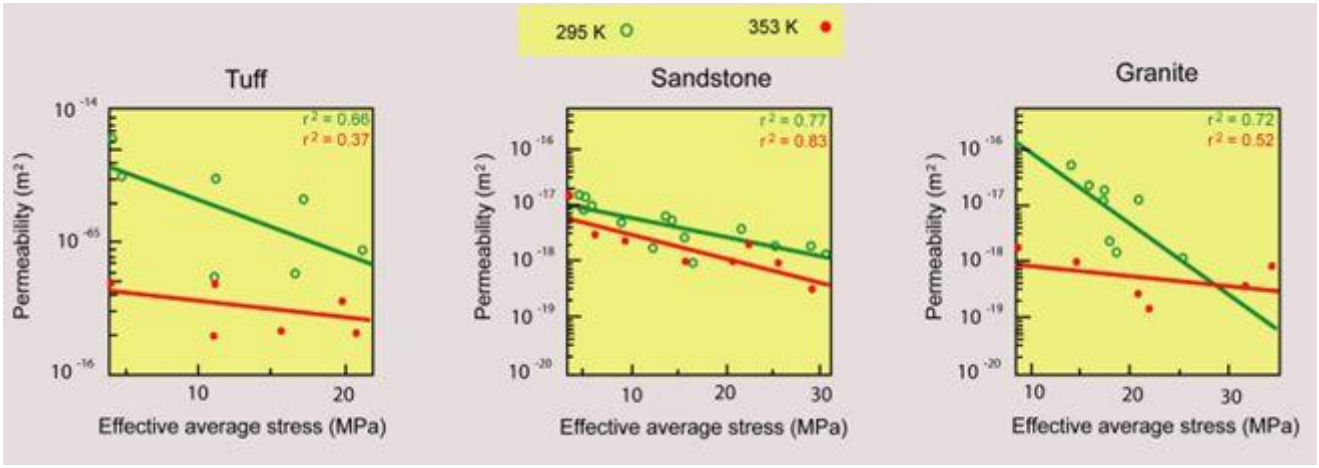

Figure 5: The relationship between post-failure permeability and effective average stress

4. SIGNIFICANCE OF TEMPERATURE- AND STRESS-DEPENDENT PERMEABILITY

The importance of stress and temperature dependency is shown by a simple 2D finite element model and full-scale model for a nuclear waste disposal cavern and applied to the underground repository for radioactive waste disposal cavern to show the sealability potential of rocks in fractured conditions. 2-D FEM (Mufundirwa *et al.*, 2011) calculated the effect of temperature, stress, and temperature-stress coupling effects on fluid inflow into a nuclear waste disposal cavern in a rock mass at 500 m deep underground (Figure 6). The rock mass was Inada granite, and the effects of temperature, stress and their interaction on fluid inflow were investigated. The reason why the software was used is that the objective of this study is not to carry out a precise thermo-hydro-mechanical numerical for a rock mass around a specific site but to demonstrate the general necessity to consider the stress and temperature dependency in the analyses of water migration around underground nuclear waste disposal caverns as stated in the introduction. Another reason is that our research group developed this software which can be fully modified to introduce stress- and temperature-dependent permeability.

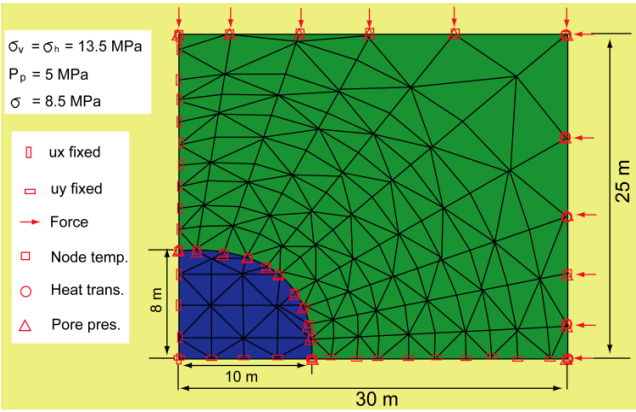

Figure 6: Underground nuclear waste disposal model

The total number of constant strain 234 triangular elements and 137 nodes were considered in this 2-D FEM. The mechanical properties used for this analysis were Young's modulus of 68 GPa, a Poisson's ratio of 0.35, a wet density of 2700 kg/m^3, an expansion coefficient of 7.94 ×10^{-6} (K^{-1}), and effective porosity of 0.60 % (Alam *et al.*, 2014). The backfill's effective porosity was 0.80%, Young's modulus was 69.4 MPa, Poisson's ratio was 0.22, wet density was 2100 kg/m^3, and the expansion coefficient was 3.10×10^{-4} (K^{-1}) (Kwon *et al.*, 2013). The pore pressure was considered 5 MPa, while the overburden pressure was supplied as 13.5 MPa hydrostatic pressure. The backfill's pore pressure was set to zero, assuming drainage. Since the rock mass is broken, the aforementioned post-failure permeability was applied. At the model's outside limits, a temperature of 295K was specified. A temperature of 353K or 295K was assigned to the edge of the backfill. The following steps calculated the elastic, isotropic, static, and steady solution:

- Steady temperature distribution.
- Static stress distribution considering thermal strain.
- Steady flow analysis considering the stress and temperature-dependency of the rock permeability and the temperature dependency of the water viscosity

At 295K, 36 to 43 MPa was the highest effective major stress at the cavern wall (Figure 7). The thermal stress first manifested under the same circumstances at a backfill boundary temperature increase of 353K, and the highest major stress ranged from 64 - 72 MPa, an average increase of 72%.

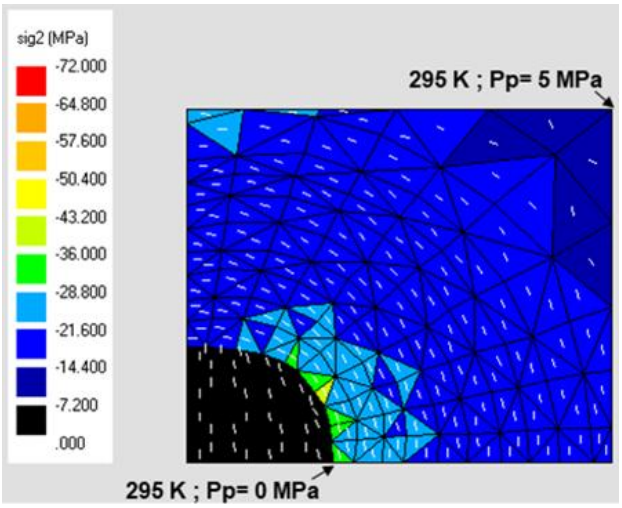

(a)

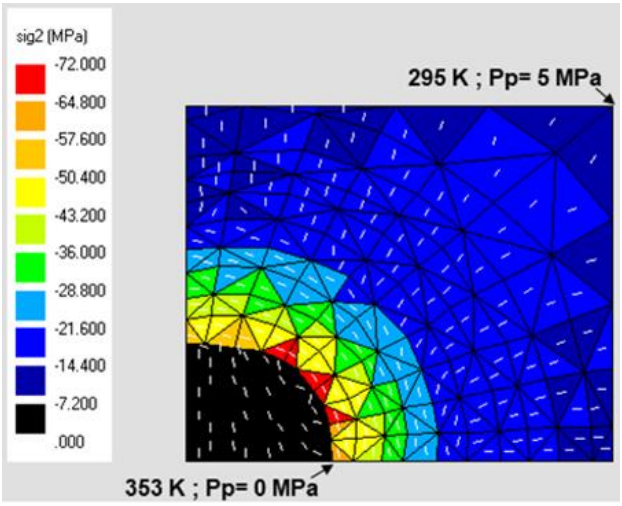

(b)

Figure 7: Maximum effective principal stress at 295 K,(a) and 353 K (b) (compression is shown as negative)

The flow rate increase was observed in the narrow area near the opening with constant *K* (Figure 8a). However, higher temperature for temperature-dependent *K* or thermal stress for stress-dependent *K* at the cavern wall slows the flow rate (Figure 10b and c). The flow rate is lower for stress- and temperature-dependent *K* (Figure 8d). The inflow into the cavern significantly decreases (1/150) with temperature-dependent *K* and more so (1/500) with stress-dependent *K* (Figure 9). When both factors are considered, the inflow is minimal (1/2000), which is the case for a radioactive disposal mining repository.

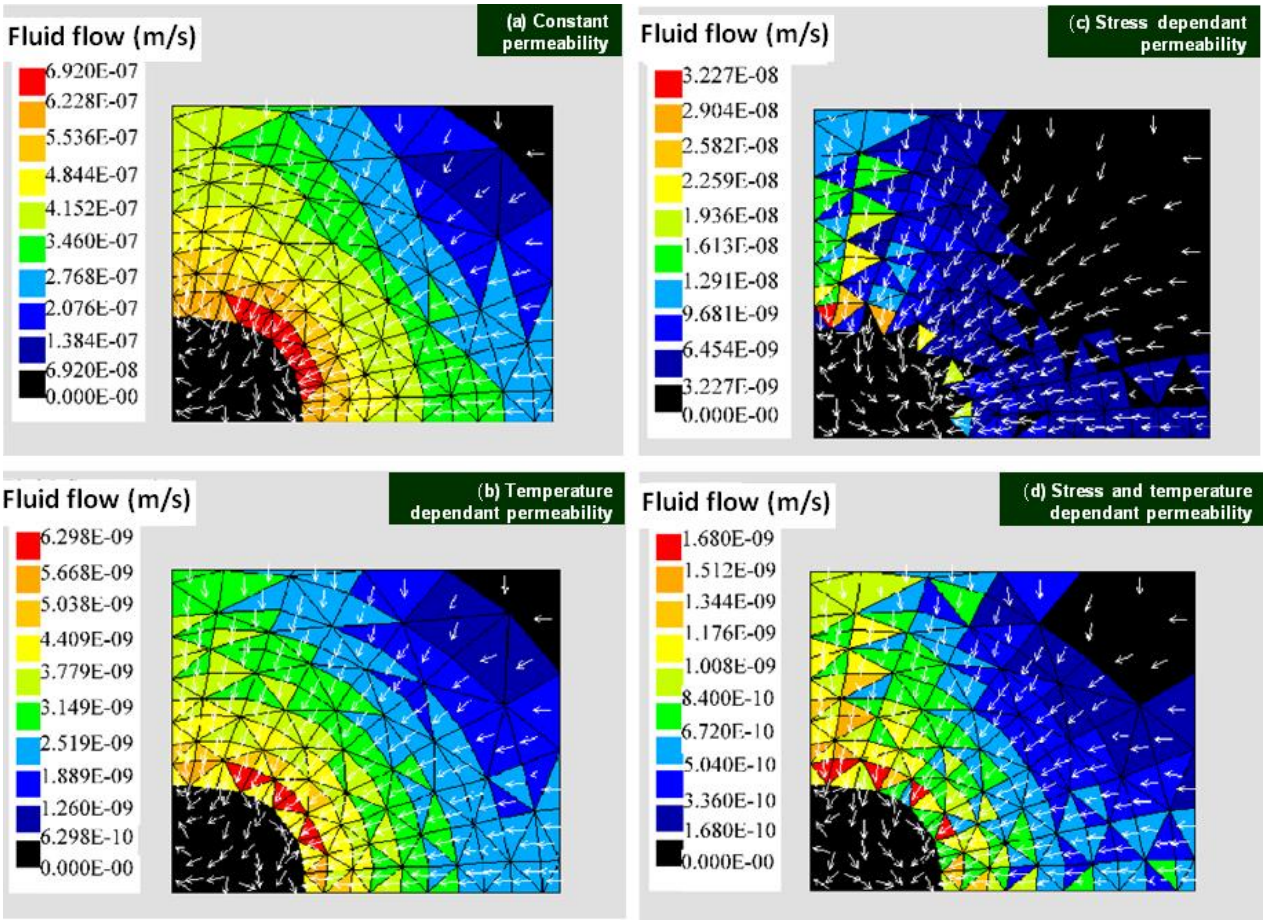

Figure 8: Flow rate distribution around the cavern considering the stress and temperature-dependent permeability

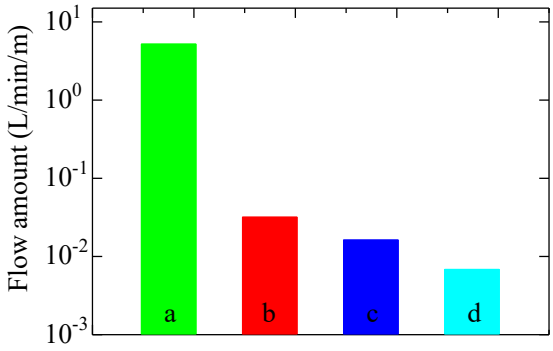

Figure 9: Inflow to the backfill (L/min/m) considering (a) no dependency, (b) temperature dependency, (c) Stress-dependency, and (d) stress and temperature dependency

5. WATER INFLOW IN UNDERGROUND NUCLEAR WASTE DISPOSAL IN ROCKS CONSIDERING STRESS AND TEMPERATURE-DEPENDENT PERMEABILITY

The most widely accepted idea for disposing of radioactive waste is to bury it deep underground. This involves putting the waste containers in a hole in the rock mass accessed by a tunnel.

The gap between the container and the hole is filled with bentonite buffer, while the tunnel is filled with broken rocks as backfill material. If groundwater seeps into the hole, it can carry radio nuclide and affect the geo-environmental condition of the area. Therefore, the flow rate around the hole is essential to assess the geo-environmental risk potential. Different rocks are being studied as possible repositories, such as granite (Canada, China, Finland), tuff (USA). This research considers granite, tuff, and sandstone rocks to evaluate their potential as mined repositories.

The model has (i) a 6×4 m^2 tunnel to access (ii) a 7×2 m^2 hole for disposal, and (iii) a 2×1 m^2 container in a 21×14 m^2 rock mass at 600 m depth (Figure 11), following the IAEA safety standards for geological disposal facilities for radioactive waste (IAEA, 2011). The total number of 2470 constant triangular elements and 1271 nodes applying the normal stress of 15 MPa at a depth of 500 m from the surface was considered in this simulation. Pore pressure gradient of 71 kPa/m was applied from the right to left boundaries. The flow rate in the rock mass along the 7 m side of the hole (Figure 11c) is compared to estimate the flow amount that could be the pathway for radio nuclide. The experimental data from Table 2 was utilized in the present study to investigate the complex relationship between the rock's permeability changes and varying levels of stress and temperature for underground excavation. The researchers were intrigued by the potential of rock masses to impede the flow of water, an essential consideration for underground geological disposal, and thus, analyzed the data extensively to extract valuable insights.

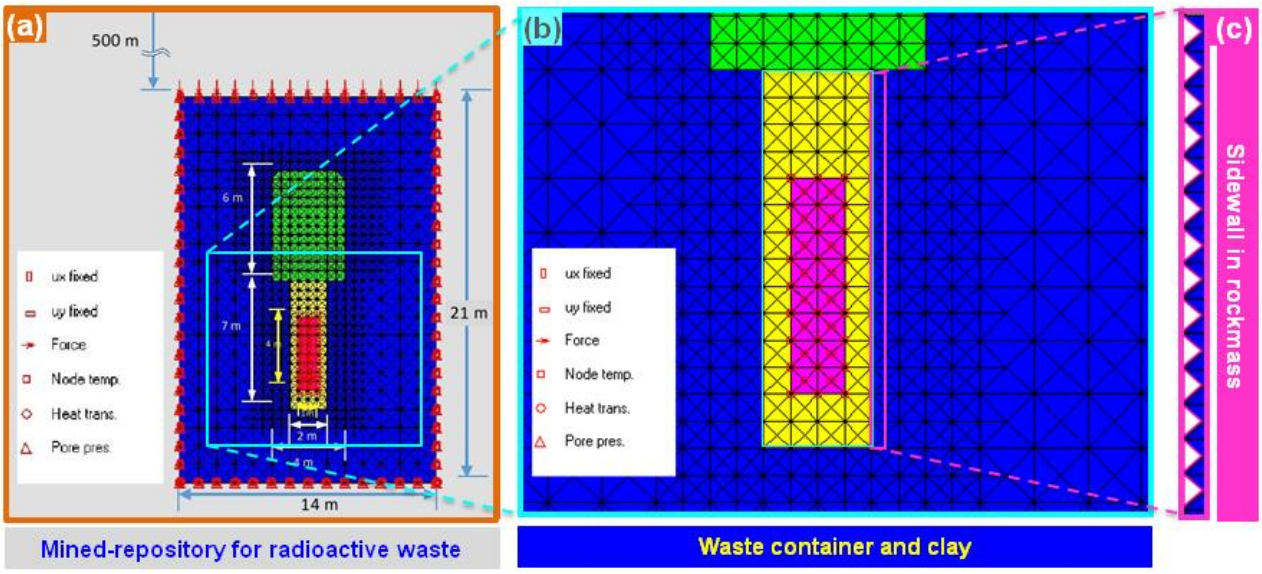

Figure 10: A model of underground disposal for radioactive waste

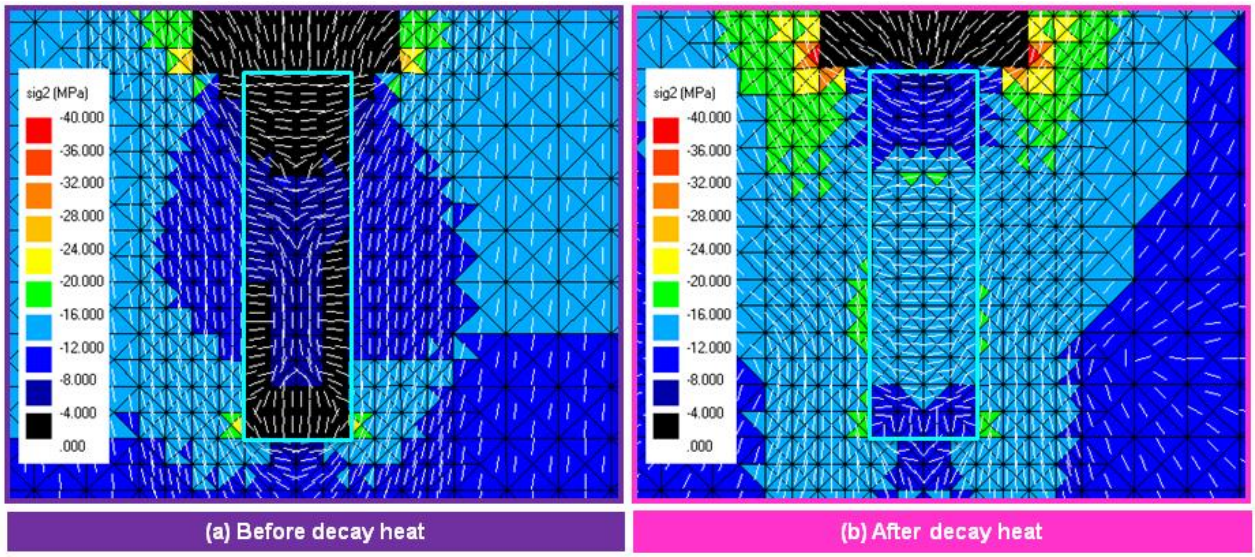

Figure 11: Temperature condition of before (a) and after (b) decay heat in the model

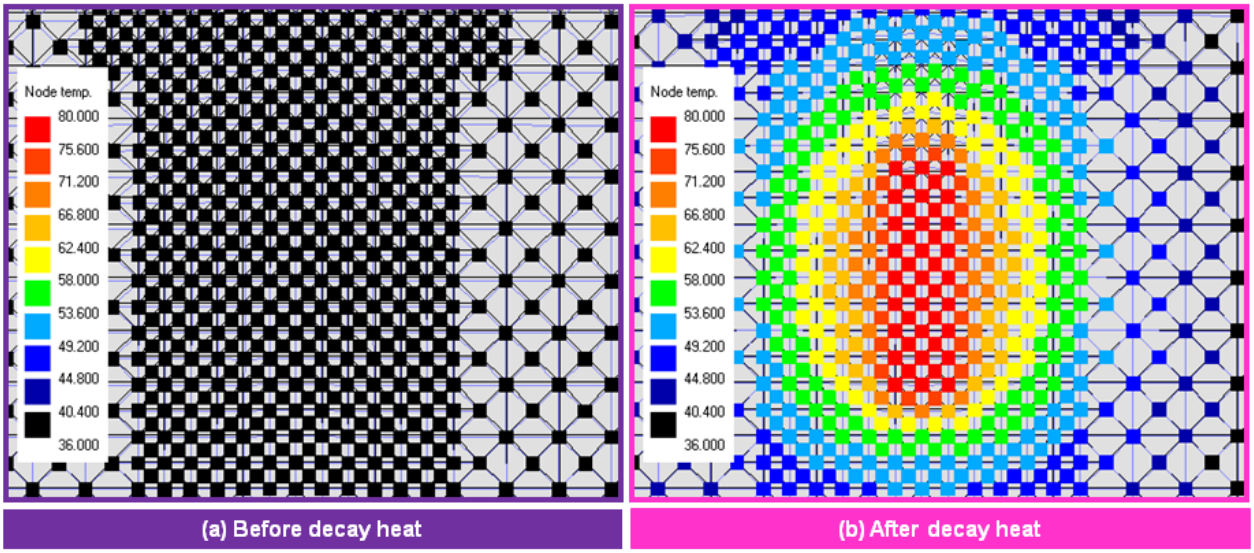

Figure 12: Major effective principal stress distribution before (a) and after (b) decay heat in granite

The analysis revealed that the temperature of the disposal area experienced a significant increase from 295 K to 353 K, as depicted in Figure 11. The consequent heat transfer throughout the rock mass was complex and multifaceted, requiring a deeper understanding of the underlying principles. The rise in temperature also engendered thermal stress, leading to a substantial increase in the effective principal stress in the granite sample. The intricate details of this relationship were elucidated in Figure 12, which demonstrated a clear increase in the stress of the rock from 8-12 MPa to 12-16 MPa. Interestingly, the rise in stress was not solely due to the thermal stress but was also attributed to the decay heat, which contributed to 38% of the stress increase.

The flow rates, both within and around the excavated repository subsequent to the decay heat, as illustrated in Figure 13. The magnitude of oscillation in the flow rate was more significant for granite and tuff as opposed to sandstone. Additionally, it was discerned that the typical flow rate for tuff outpaced that of granite and sandstone, while the latter displayed the most modest average flow rate.

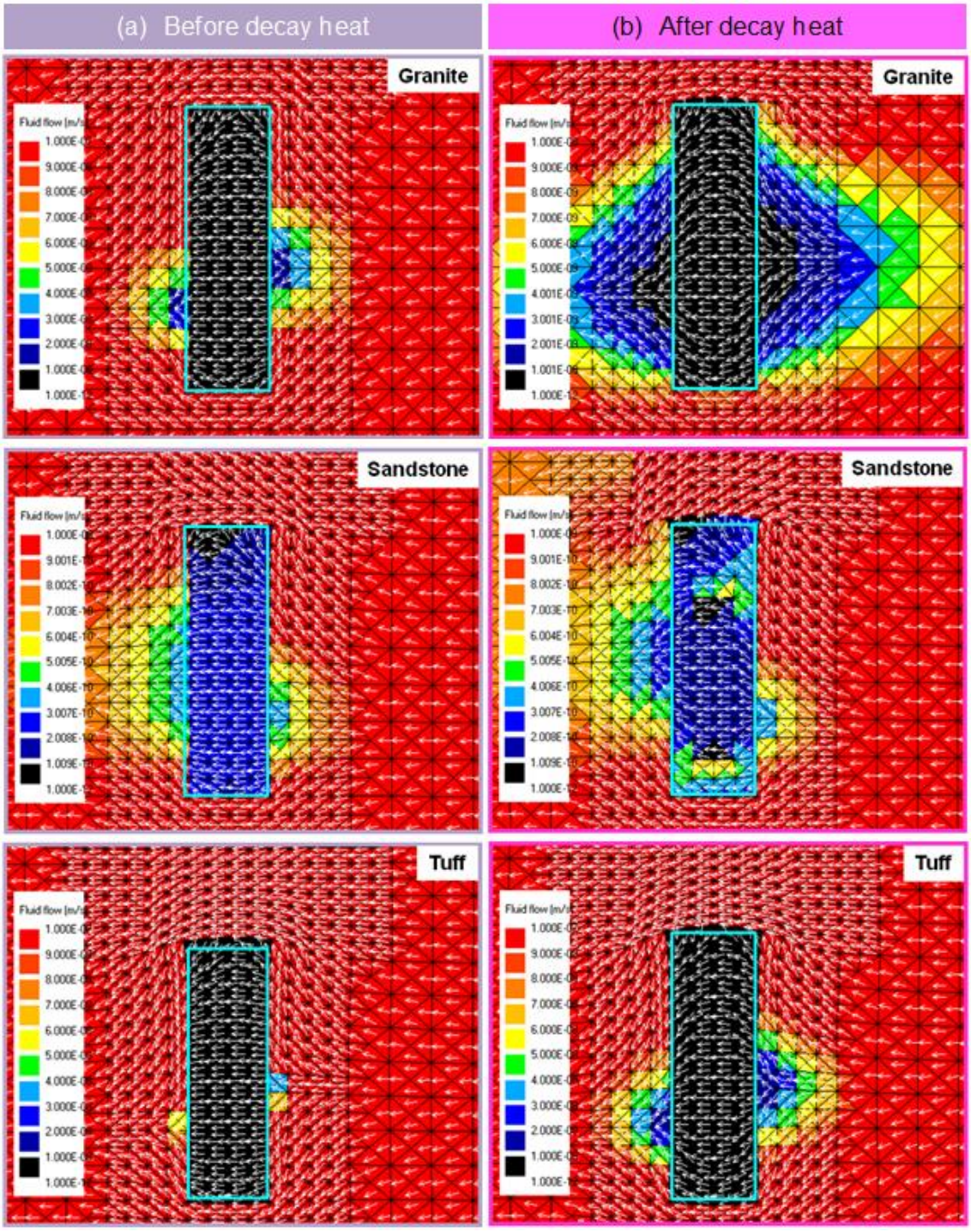

Figure 13: Fluid flow velocity around the depository before (a) and after (b) decay heat in rockmass, considering the stress and temperature dependant permeability

The results of the simulation were found to be rather intriguing. Specifically, it was noted that the flow rate of tuff, when subjected to higher temperatures, appeared to be lower in comparison to when it was placed under lower temperature conditions. As per the gathered data, the average flow rate of tuff along the sidewall showed a reduction of a whopping 73%, which is rather significant, as depicted in Figure 10c. Interestingly, granite displayed a considerable decrease in its average flow rate when the temperature was increased from 295K to 353K (Figure 14). The recorded data showcased a decline from 1.34×10^{-7} m/s to 1.91×10^{-9} m/s, which translated to a massive 99% drop in flow rate. In contrast, the average flow rate of sandstone was almost the same at both temperatures. It is imperative to note that tuff demonstrated the highest flow rate when compared to the other two types of rocks, both at higher and lower temperatures. Furthermore, sandstone presented the lowest flow rate among the three. However, at a temperature of 353K, sandstone and granite showcased relatively similar flow rates.

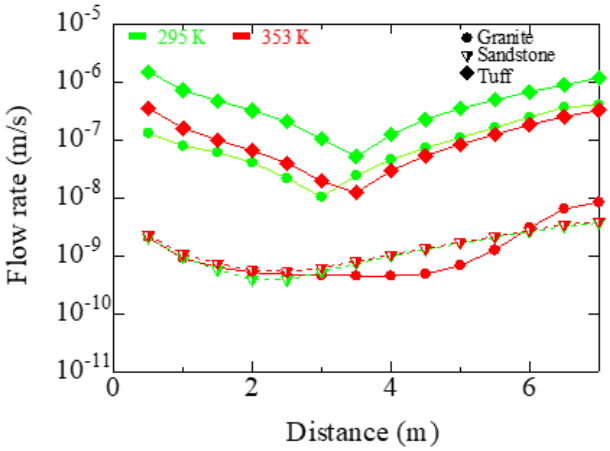

Figure 14: Fluid velocity in the sidewall before and after decay heat, considering the dependency of stress and temperature on permeability

6. DISCUSSION

The investigation of mathematical modeling for hydrothermal convection encompassing a radioactive waste depository in hard rock has piqued the interest of numerous researchers. Hodgkinson's research in 1980 served as a catalyst for further examination in this domain, with several research publications delving into this topic. Zhang *et al.* (2011) brought forth the test case 2 results of an exercise concerned with mathematical modeling for hydrothermal convection, while Liu *et al.* (2015) delved into the impact of compressive creep deformation on gas permeability of the porous argillite. Daniels *et al.* (2017) found that hydraulic properties of bentonite are exceedingly sensitive to thermal loading and the category of imposed boundary condition. Philipp *et al.* (2017) delved into microstructural controls on permeability for various facies of OPA.

Urpi *et al.* (2019) scrutinized the repercussions of thermal pressurization throughout the lifespan of a deep geological repository (DGR) for high-level radioactive waste. Plúa *et al.* (2021) explored the Thermo-Hydro-Mechanical (THM) responses of a porous rock with low permeability under thermal loading within the context of deep geological disposal of radioactive waste. Onoe *et al.* (2021) investigated the methodology of modeling for fractured granite around the drift at a depth of 500 m in the Mizunami Underground Laboratory, Japan, as a case study. Ogata *et al.* (2021) advanced a groundbreaking framework for coupled THMC analysis employing explicit rock fracture. Sellin *et al.* (2013) made valuable contributions to this field with their work.

Collectively, these investigations concentrate on diverse facets of mathematical modeling for hydrothermal convection around radioactive waste depositories in hard rock. They involve the influence of multiple factors on hydraulic properties, permeability, and thermal pressurization, as well as the methodology of modeling for fractured granite. These previous researches contribute substantially to the scholarly discourse and comprehension of the complex and interdisciplinary field of nuclear waste disposal. The current investigation places a paramount focus on the intricate interplay between stress and temperature-dependent permeability of post-compression. This crucial facet of permeability, intriguingly, has been woefully disregarded in all antecedent inquiries concerning this subject matter. It is crucial to note that the nature of this intricate interplay is yet to be fully comprehended, and as such, further investigations are deemed necessary.

In the experimental results (Figure 2), the post-failure permeability negatively correlated with average effective stress. The negative correlation is because the aperture of the water paths closed with stress. The post-failure permeability at 353K was lower than 295K for all rocks. The decrease would be due to the further decrease in the aperture of the water paths by the more viscous deformation of mineral particles under the higher temperature.

However, the stress and temperature effects on the post-failure permeability differ for each rock type. The difference might be explained by considering the permeability of the rock matrix. For example, the high permeability of the porous glass matrix of the tuff at 353K did not decrease with stress because the water paths were almost closed, and water flowed in the matrix (Figure 3a). The permeability of the granite matrix is very low so that the permeability of the rock at 295K was significantly ruled by the aperture of the water paths which varied with stress (Figure 3c).

The water inflow significantly decreased in the numerical analysis results for the simple cavern model (Figure 8), considering the stress and temperature dependencies of permeability in the calculation (Figure 9) for granite. The decrease is due to stress concentration, thermal stress, and temperature rise, which means the sealability of underground nuclear waste disposal caverns may be higher than usually expected, at least at the early stages of the storage. Therefore, introducing stress and temperature-dependent permeability could contribute to the thoughtful design of those disposal sites.

Based on the outcomes, a full-scale model was considered for granite, sandstone, and tuff. For granite, the decrease in flow amount (Figure 15) at increased temperature was found as it was for the simple cavern model (Figure 9). The permeability of the granite matrix is very low, so the permeability of the rock was significantly ruled by the aperture of the rupture planes, which decreased at increased temperature (Figure 3c). The decrease was because of the more viscous deformation of mineral particles under high temperatures. For sandstone, the flow amount was not so different for increased temperature and was almost equal to that for granite. The viscoplastic deformation of cementing material of the sandstone was not enough to close the flow path (Figure 3b) at the temperature. For tuff, the flow amount slightly decreased at the increased temperature where pores were available for water migration at the temperature (Figure 3c).

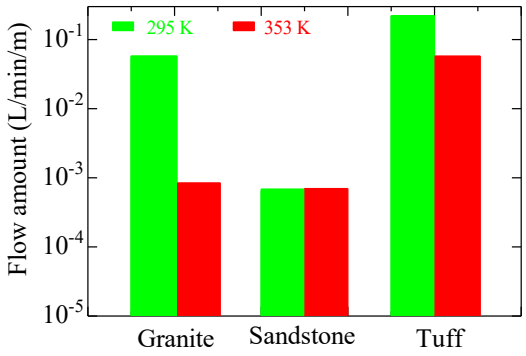

Figure 15: Fluid amount in the sidewall before and after decay heat, considering the dependency of stress and temperature on permeability

7. CONCLUSIONS

To demonstrate the necessity to consider the stress and temperature-dependency in permeability, equations that represent the post-failure permeability as a function of average effective stress and temperature were proposed. For a simple underground nuclear waste disposal cavern, the water inflow was predicted using a 2-D elastic FEM with or without the stress and temperature dependency into account for granite. The results showed that the fractured rock permeability near the cavern became lower due to stress concentration, thermal stress, and temperature rise, and water inflow became significantly less for granite, which demonstrates that the introduction of the stress and temperature-dependent permeability could contribute to the thoughtful design of those disposal sites.

Among the three rocks for a full-scale underground radioactive disposal site in granite, sandstone, and tuff considering the stress and temperature-dependent permeability, a high sealability could be expected for granite and sandstone but not for the tuff.

The conclusion in this study was obtained, of course, from the limited rock types and conditions. Extensive experiments under various conditions for various types of rock may be needed. The stress and temperature-dependent permeability concept should be introduced for a wide variety of more practical scenarios, such as a transient analysis for the water migration around a cavern constructed in a rock mass with a hydraulic gradient.

ACKNOWLEDGEMENTS

Authors would like to express their gratitude to the Department of Petroleum and Mining Engineering, Military Institute of Science and Technology, Dhaka, Bangladesh; Faculty of Engineering, Hokkaido University, Sapporo, Japan; Research Unit of Materials Science and Structure, Institute of Technology of Cambodia, Phnom Penh, Cambodia; and School of Civil Engineering, Universiti Teknologi Malaysia, Johor Bahru, Malaysia.

REFERENCES

Alam, B., Fujii, Y., Fukuda, D., Kodama, J., & Kaneko, K. (2015). Fractured Rock Permeability as a Function of Temperature and Confining Pressure. *Pure and Applied Geophysics*, 172, 2871-2889. DOI: https://doi.org/10.1007/s00024-015-1073-2

Alam, B., Niioka, M., Fujii, Y., Fukuda, D., & Kodama, J. (2014). Effects of Confining Pressure on the Permeability of Three Rock Types under Compression. *International Journal of Rock Mechanics and Mining Sciences*, 65, 49-61. DOI: https://doi.org/10.1016/j.ijrmms.2013.11.006

Bian, H. B., Jia, Y., Armand, G., Duveau, G., & Shao, J. F. (2012). 3D numerical modelling thermo-hydromechanical behaviour of underground storages in clay rock. *Tunneling and Underground Space Technology*, 30, 93-109. DOI: https://doi.org/10.1016/j.tust.2012.02.011

Brace, WF., Walsh, JB., & Frangos, WT. (1968). Permeability of granite under high pressure. *Journal of Geophysical Research* 73,2225–2236. DOI:https://doi.org/10.1029/JB073i006p02225

Dhakal, G., Yoneda, T., Kato, M., & Kaneko, K. (2002). Slake durability and mineralogical properties of some pyroclastic and sedimentary rocks. *Engineering Geology*, 65, 31–45. DOI: https://doi.org/10.1016/S0013-7952(01)00101-6

Doi, S. (1963). Petrological and petrochemical studies of welded tuff. *Report of Geological Survey Hokkaido*, 29, 30–103.

IAEA (2011). *Geological disposal facilities*. Vienna: International atomic energy agency.

Kwon, S., Cho, WJ., & Lee JO. (2013). An analysis of the thermal and mechanical behavior of engineered barriers in a high-level radioactive waste repository. Nuclear engineering and Technology, 45(1), 41-52. DOI: https://doi.org/10.5516/NET.06.2012.015

Lin, W., & Takahashi, M. (2008). Anisotropy of strength and deformation of Inada granite under uniaxial tension. *Chinese Journal of Rock Mechanics and Engineering*, 12, 2463–72.

Mufundirwa, A., Fujii, Y., Kodama, N., & Kodama, J. (2011). Analysis of natural rock slope deformations under temperature variation: A case from a cool temperate region in Japan. *Cold Regions Science and Technology*, 65 (3), 488-500. DOI: https://doi.org/10.1016/j.coldregions.2010.11.003

Yu, L., Chen, G. J., & Weetjens, E. (2017). A solution around a backfilled cavity in a low-permeability poroelastic medium with application in in situ heating tests. *International Journal of Numerical Analysis Methods in Geomechanics*, 41(3), 3-29. DOI: https://doi.org/10.1002/nag.2542

Daniels, K. A., Harrington, J. F., Zihms, S. G., & Wiseall, A. C. (2017). *Bentonite permeability at elevated temperature*. Geosciences (Switzerland), 7(1). DOI: https://doi.org/10.3390/geosciences7010003

Hodgk1nson, D. P. (1980). *A mathematical model for hydrothermal convection around a radioactive waste*

depository in hard rock. In Annals of Nuclear Energy (Vol. 7). Pergamon Press Ltd.

Liu, Z., Shao, J., Xie, S., & Secq, J. (2015). Gas permeability evolution of clayey rocks in process of compressive creep test. *Materials Letters*, 139, 422–425. DOI: https://doi.org/10.1016/j.matlet.2014.10.139

Ogata, S., Maeda, Y., Fukuda, D., Yasuhara, H., Inui, T., & Kishida, K. (2021). A novel framework for coupled THMC analysis employing explicit rock fracture. *IOP Conference Series: Earth and Environmental Scie*nce, 861(3). DOI: https://doi.org/10.1088/1755-1315/861/3/032053

Onoe, H., Ishibashi, M., Ozaki, Y., & Iwatsuki, T. (2021). Development of modeling methodology for hydrogeological heterogeneity of the deep fractured granite in Japan. *International Journal of Rock Mechanics and Mining Sciences*, 144. DOI: https://doi.org/10.1016/j.ijrmms.2021.104737

Philipp, T., Amann-Hildenbrand, A., Laurich, B., Desbois, G., Littke, R., & Urai, J. L. (2017). The effect of microstructural heterogeneity on pore size distribution and permeability in Opalinus Clay (Mont Terri, Switzerland): Insights from an integrated study of laboratory fluid flow and pore morphology from BIB-SEM images. *Geological Society Special Publication*, 454 (1), 85–106. Geological Society of London. DOI: https://doi.org/10.1144/SP454.3

Plúa, C., Vu, M. N., Armand, G., Rutqvist, J., Birkholzer, J., Xu, H., Guo, R., Thatcher, K. E., Bond, A. E., Wang, W., Nagel, T., Shao, H., & Kolditz, O. (2021). A reliable numerical analysis for large-scale modelling of a high-level radioactive waste repository in the Callovo-Oxfordian claystone. *International Journal of Rock Mechanics and Mining Sciences*, 140. DOI: https://doi.org/10.1016/j.ijrmms.2020.104574

Sellin, P., & Leupin, O. X. (2014). The use of clay as an engineered barrier in radioactive-waste management - A review. *Clays and Clay Minerals*, 61(6), 477–498. DOI: https://doi.org/10.1346/CCMN.2013.0610601

Urpi, L., Rinaldi, A. P., Rutqvist, J., & Wiemer, S. (2019). Fault Stability Perturbation by Thermal Pressurization and Stress Transfer Around a Deep Geological Repository in a Clay Formation. *Journal of Geophysical Research: Solid Earth*, 124(8), 8506–8518. DOI: https://doi.org/10.1029/2019JB017694

Zhang, K., Croisé, J., & Mayer, G. (2011). Computation of the Couplex-Gaz exercise with TOUGH2-MP: Hydrogen flow and transport in the pore water of a low-permeability clay rock hosting a nuclear waste repository. *Nuclear Technology*, 174(3), 364–374. DOI: https://doi.org/10.13182/NT11-A11746